Received: 10 August 2022 | Revised: 16 November 2022 | Accepted: 12 December 2022

DOI: 10.1002/ddr.22030

RESEARCH ARTICLE

DRUG DEVELOPMENT RESEARCH WILEY

Two new alkaloids from *Dendrobium nobile* Lindl. exhibited neuroprotective activity, and dendrobine alleviated $A\beta_{1-42}$-induced apoptosis by inhibiting CDK5 activation in PC12 cells

Cheng-Chen Zhang[1,2] | Yan-Li Kong[1] | Mao-Sheng Zhang[1] | Qin Wu[1] | Jing-Shan Shi[1]

[1]Key Laboratory of Basic Pharmacology of Ministry of Education and Joint International Research Laboratory of Ethnomedicine of Ministry of Education, School of Pharmacy, Zunyi Medical University, Zunyi, China

[2]State Key Laboratory of Functions and Applications of Medicinal Plants, Guizhou Medcial University, Guiyang, China

Correspondence
Jing-Shan Shi, Key Laboratory of Basic Pharmacology of Ministry of Education and Joint International Research Laboratory of Ethnomedicine of Ministry of Education, School of Pharmacy, Zunyi Medical University, Zunyi 563000, China.
Email: zmcshijs@163.com

Funding information
Guizhou Science and Technology Department; State Key Laboratory of Functions and Applications of Medicinal Plants, Guizhou Medicial University

Abstract

Dendrobium nobile Lindl. is registered in the Chinese Pharmacopoeia as a traditional medicine. Phytochemical investigation of the ethanol extract of *D. nobile* Lindl. stems yielded three alkaloid compounds, including two new compounds dendroxine B (**2**) and denrine B (**3**) as well as one known compound dendrobine (**1**). Here, we identified the structure of these compounds using spectroscopic analyses and compared them with those described in previous studies. Compounds **1**–**3** were found to show protective effect against amyloid-β 1–42 ($A\beta_{1-42}$)-induced neurotoxicity in rat pheochromocytoma (PC12) cells, among which dendrobine exhibited the most significant neuroprotective effect. Hoechst 33342/propidium iodide staining indicated that dendrobine ameliorated $A\beta_{1-42}$-induced apoptosis. Moreover, quantitative real-time polymerase chain reaction and western blot analysis analysis demonstrated that dendrobine suppressed the activation of cyclin-dependent kinase 5 (CDK5), upregulated Bcl-2 expression, and downregulated Bax, cyto-c, and caspase-3 expression. Molecular docking analysis and surface plasmon resonance assay suggested that dendrobine directly bound to CDK5 protein with a KD value of 2.05×10^{-4} M. In summary, alkaloids are the neuroprotective constituents of *D. nobile* Lindl., and dendrobine protected PC12 cells against $A\beta_{1-42}$-induced apoptosis by inhibiting CDK5 activation.

KEYWORDS
Alzheimer's disease, apoptosis, *Dendrobium nobile* Lindl. alkaloids

1 | INTRODUCTION

Alzheimer's disease (AD), a common neurodegenerative disease characterized by cognitive impairment, imposes an enormous burden on society (Long & Holtzman, 2019). Extracellular Aβ-containing senile plaque and intracellular tau-containing neurofibrillary tangles are the neuropathological profiles of AD (Long & Holtzman, 2019). The major species of Aβ produced by cells are $A\beta_{40}$ (80%–90%) and $A\beta_{42}$ (5%–10%) (Miranda et al., 2021). In AD brains, Aβ monomers aggregate into oligomers, protofibrils, and insoluble amyloid

This is an open access article under the terms of the Creative Commons Attribution License, which permits use, distribution and reproduction in any medium, provided the original work is properly cited.
© 2023 The Authors. *Drug Development Research* published by Wiley Periodicals LLC.

fibrils (Michaels et al., 2020). Soluble Aβ oligomers exert deleterious effects in AD, and $A\beta_{42}$ oligomers are considered especially neurotoxic (Madhu & Mukhopadhyay, 2021). The NMDAR antagonist memantine, at proper concentration, preferentially blocks pathologically-stimulated extrasynaptic NMDARs over physiologically-activated synaptic NMDARs, and partially ameliorates Aβ-induced synaptic toxicity and cognitive deficit (Tu et al., 2014). Despite the progress in partially clarifying the underlying pathobiology of AD, disease-modifying therapies for AD are currently unavailable (Cummings et al., 2021). Novel therapeutic drugs are still being actively developed.

Apoptosis is correlated with the progression of AD, and cell survival in AD is governed by pro and antiapoptotic mechanisms (Sharma et al., 2021). Apoptosis is mediated by two pathways, intrinsic and extrinsic. The interaction between Bcl-2 and Bax facilitates the release of cytochrome c (cyto-c) in the intrinsic apoptotic pathway (Sharma et al., 2021). Caspase-3 is critical for apoptosis and associated with synaptic failure in AD (Quntanilla & Tapia-Monsalves, 2020). Cyclin-dependent kinase 5 (CDK5) is a key component of central nervous system development, included in neuronal differentiation, synaptic functions, and memory consolidation. Indeed, dysregulated CDK5 activity contributes to the pathogenesis of tau hyperphosphorylation, neurofibrillary tangles formation and neuronal apoptosis in AD (Lu et al., 2019; Y. L. Zhang, Linghu, et al., 2021; Y. Zhang, Zhang, et al., 2021). Inhibition of CDK5 activity was shown to protect from neuronal cell loss by suppressing Aβ-induced neurotoxicity (S. L. Liu et al., 2016).

Dendrobium nobile Lindl. is a traditional medicine that is registered in the Chinese Pharmacopoeia. Main active constituents of *D. nobile* Lindl. are alkaloids, polysaccharides (Wang, 2021). *D. nobile* Lindl. alkaloids (DNLA) have numerous pharmacological effects, including neuroprotection, hepatoprotection, blood sugar and lipid reduction, and antitumor effects (Li et al., 2022; Nie et al., 2020). However, the effects and mechanisms against AD of alkaloid compounds from *D. nobile* Lindl. are still unclear. Here, we isolated and identified alkaloid compounds from a 95% ethanol (EtOH) extract of *D. nobile* Lindl. stems, and investigated the effects of these compounds on $A\beta_{1\text{-}42}$-induced neurotoxicity in PC12 cells, as well as underlying mechanism.

2 | MATERIALS AND METHODS

2.1 | Chemistry

2.1.1 | General experimental procedures

Optical rotations were conducted using an API/1 W automatic polarimeter (Rudolph). UV spectra were collected on a UV-2401 PC spectrophotometer (Shimadzu). Electronic circular dichroism (ECD) spectrum was measured on a Chirascan V100 circular dichroism spectrometer (Applied Photophysics Limited). IR spectra were collected on a Nicolet iS10 FT-IR spectrometer (Thermo Scientific). NMR spectra were measured on a DRX 500 NMR spectrometer (Bruker). HR-ESIMS were performed on a LCMS-IT-TOF (Shimadzu).

2.1.2 | Plant material

D. nobile Lindl stems were obtained from Chishui Xintian Traditional Chinese Medicine Inc. (Zunyi) and were authenticated by Professor Shi Jing-Shan from Zunyi Medical University, Guizhou, China. A voucher specimen (No. 20180912) was deposited with the Herbarium of the School of Pharmacy, Zunyi Medical University.

2.1.3 | Extraction and isolation

The air-dried stems of *D. nobile* Lindl (3 kg) were reflux extracted with 95% EtOH (15 L × 1 h, three times). The EtOH extract (786 g) was suspended in hydrochloric acid solution (pH 3), filtered, and partitioned with petroleum ether to remove impurities. The acidic solution was separated by a cation exchange resin column chromatography, and eluted successively with distilled water, 80% EtOH, and 80% alkaline-EtOH (adjusted to pH 10 with ammonia) to afford three fractions A–C. Next, fraction C (19 g) was eluted upon Sephadex LH-20 ($CHCl_3$-MeOH, 1:1) to give DNLA (15 g). DNLA were dissolved in acetone and then recrystallized at 4°C to obtain compound **1** (8 g). After recrystallization of DNLA, the mother liquor was concentrated to yield one fraction C-1. Subsequently, fraction C-1 (1.2 g) was subjected to column chromatography (CC) (silica gel, 80-100 mesh; petroleum ether-acetone 8:1 → 7:1 → 5:1 → 3:1) to afford three subfractions, C-1-1 to C-1-3. The subfraction C-1-1 (20 mg) was separated by silica gel CC (200–300 mesh) using petroleum ether/EtOAc (10:1) to afford compound **2** (4 mg). The subfraction C-1-2 (100 mg) was separated by silica gel CC (200–300 mesh) eluted with petroleum ether/EtOAc (8:1) to obtain compound **3** (30 mg).

2.2 | Pharmacology

2.2.1 | Chemicals and reagents

$A\beta_{1\text{–}42}$ peptide and memantine hydrochloride were supplied by Sigma-Aldrich Co. Bcl-2 antibody (ab196495) and phospho-CDK5/Tyr15 antibody (ab133463) were ordered from Abcam Co. Bax antibody (#2772), cyto-c antibody (#4272), caspase-3 antibody (#9662), CDK5 antibody (#2506), GAPDH antibody (#2118) and horseradish peroxidase-linked secondary antibody (#7074) were ordered from Cell Signaling Technology Inc.

2.2.2 | Cell culture and treatment

PC12 cell line (CRL-1721) was obtained from American Type Culture Collection. PC12 cells were cultured in RPMI-1640 (Gibco) supplemented with 10% horse serum (HS; Gibco), 5% fetal bovine serum (FBS; Gibco) and 2 mM L-glutamine (Gibco) under 5% CO_2 at 37°C. The cells were incubated with 100 ng/ml NGF for 5 days to induce differentiation. The differentiated PC12 cells were cultured in DMEM with high glucose (Gibco) and 10% FBS in a 5% CO_2 incubator at 37°C.

$A\beta_{1-42}$ was dissolved in PBS at 2 mM and incubated for 5 days at 37°C to aggregate into fibrils before use (Ospondpant et al., 2022). To assess the cytotoxicity of compounds **1**–**3**, PC12 cells were treated with 0.001, 0.01 and 0.1 μM of indicated compounds for 36 h. To investigate the neuroprotective effect and mechanism of compounds **1**–**3**, PC-12 cells were pretreated with indicated compounds (0.001, 0.01, and 0.1 μM) or memantine hydrochloride (0.1 μM) as a positive control for 12 h, and co-incubated with 20 μM $A\beta_{1-42}$ for another 24 h. Blank control group contained untreated cells.

2.2.3 | Cell viability assay

Briefly, PC12 cells were seeded into 96-well microplates at 2000 cells per well before exposure to compounds **1**–**3** as described above. The cell viability was measured using a cell counting kit-8 (CCK-8; Solarbio) assay as reported (Z. Zhang et al., 2019).

2.2.4 | Cell morphology

PC12 cells were inoculated in 24-well plates at 2×10^4 cells per well before exposure to dendrobine as outlined above. Cell morphology was observed, and cell images were taken as described previously (Alghazwi et al., 2019).

2.2.5 | Hoechst 33342/PI double staining

PC12 cells were inoculated in six-well plates at 2×10^5 cells per well before exposure to dendrobine as described above. After treatment, the rate of cell apoptosis was determined using a Hoechst 33342/PI staining assay kit (Solarbio) as described (Zeng et al., 2020). Photographs were taken by an inverted fluorescence microscope (IX73; Olympus).

2.2.6 | Quantitative real-time polymerase chain reaction (qRT-PCR)

PC12 cells (1×10^6 cells/well) were seeded into six-well plates before exposure to dendrobine as outlined above. Total RNA was isolated from the cell samples using an RNA extraction kit (Beyotime). Next, the RNA was reversely transcribed using a complementary DNA (cDNA) synthesis kit (Beyotime). cDNA templates were amplified and quantified using SYBR Green qPCR Mix (Beyotime) on a CFX Connect qRT-PCR system (Bio-Rad). The messenger RNA (mRNA) expressions were calculated with $2^{-\Delta\Delta C_t}$ method and normalized to *GAPDH* (Hu et al., 2019) Table 1.

2.2.7 | Western blot analysis

PC12 cells (1×10^6 cells/well) were seeded into six-well plates before exposure to dendrobine as outlined above. After treatment, the cells were dissolved with RIPA buffer. Protein extraction and quantification, 10%–12% SDS-PAGE, and immunoblot analysis were performed as described (Yang, Wu, et al., 2020).

2.2.8 | Molecular docking

Molecular docking analysis was conducted between dendrobine and human CDK5 using AutoDock 4.2.6 software. The CDK5 protein structure (PDB ID: 7VDP) was prepared using AutoDockTools 1.5.6, which included adding polar hydrogens, calculating charges and combining non-polar hydrogens. The docking grid box was set at center 55.647, −36.693, and 52.879 Å in x, y, and z coordinates, and the dimension size of grid box was 30 × 20 × 20 points. The docking was conducted using Lamarckian Genetic Algorithm. The best-scored pose was analyzed using Discovery Studio 3 and PyMol software for the interaction between dendrobine and human CDK5.

TABLE 1 Primer sequences for qRT-PCR experiments

Gene	Forward primers	Reverse primers
Bcl-2	5′-TGGAGAGCGTCAACAGGGAGATG-3′	5′-GTGCAGATGCCGGTTCAGGTAC-3′
Bax	5′-AGACACCTGAGCTGACCTTGGAG-3′	5′-TTCATCGCCAATTCGCCTGAGAC-3′
Cyto-c	5′-AAAGGAGGCAAGCATAAGACTGGAC-3′	5′-ACCTTTGTTCTTGTTGGCATCTGTG-3′
caspase-3	5′-GCGGTATTGAGACAGACAGTGGAAC-3′	5′-AACCATGACCCGTCCCTTGAATTTC-3′
Cdk5	5′-CTGCTAGGGACACCGACTGAGG-3′	5′-GCATTGAGTTTGGGCACGACATTC-3′
GAPDH	5′-ACGGCAAGTTCAACGGCACAG-3′	5′-CGACATACTCAGCACCAGCATCAC-3′

2.2.9 | Surface plasmon resonance assay

The binding affinity of dendrobine to human CDK5 protein was evaluated by surface plasmon resonance (SPR) assay using a Biacore X100 instrument (GE Healthcare). 40 μg ml^{-1} of CDK5 protein (Sino Biological Inc.) was dissolved in 10 mM sodium acetate (pH 4.0) and immobilized onto a CM5 sensor chip using Amine method. Dendrobine was diluted at 1.5625, 3.125, 6.25, 12.5, 25, 50, and 100 μM with PBS-P buffer. All the measurements were performed in PBS-P buffer at 25°C. Dendrobine and CDK5 protein were allowed to associate for 90 s and then dissociate for 120 s. After dissociation, the sensor chip was regenerated with Glycine-HCl (pH 3.0; GE Healthcare). Equilibrium dissociation constant (K_D) was evaluated by global fitting with a 1:1 Langmuir binding model using the Biacore Evaluation software (GE Healthcare).

2.2.10 | Statistical analysis

Data were reported as mean ± SEM. Statistical analysis of differences between groups was performed using one-way analysis of variance with Dunnett's test. $p < .05$ were considered significant.

3 | RESULTS

3.1 | Structure of compounds 1–3

Two new compounds dendroxine B (**2**), denrine B (**3**), and one known compound dendrobine (**1**) (M. S. Zhang, Linghu, et al., 2021; Y. Zhang, Zhang, et al., 2021), were isolated from the EtOH extract of *D. nobile* Lindl. stems (Figure 1).

Compound **2** had a molecular formula of $C_{16}H_{23}NO_2$ based on HR-ESI-MS $[M + Na]^+$ (*m/z* 284.1622, calcd. 284.1621). The ^1H, ^{13}C and HSQC NMR spectroscopic data of compound **2** demonstrated 16 signals, including four quaternary carbons (one carbonyl carbon, 196.7 ppm), four methines, five methylenes and three methyls (Table 2). The spectroscopic data suggested that compound **2** was similar to dendroxine, one of alkaloids isolated from *D. nobile* Lindl. (Yang, Wu, et al., 2020). The COSY correlation from H-15 to H-16, along with the HMBC correlations from H-15 to C-2, C-11, C-16

TABLE 2 ^1H and ^{13}C NMR data of compound **2** (δ in ppm, *J* in Hz)

Position	δ_H	δ_C
1		56.6
2		106.4
3		196.7
4		141.1
5	6.43, d (4.8)	141.0
6	2.47, m	50.1
7	1.73, m	32.7
	2.00, m	
8	1.67, m	33.6
	1.79, m	
9	2.39, m	49.7
10	1.29, s	23.2
11	2.83–2.86, m	62.2
12	2.81, m	27.0
13	1.00, d (6.9)	21.8
14	1.04, d (6.9)	21.9
15	2.98, ddd (8.5, 8.7, 12.2)	52.0
	3.03, ddd (2.7, 6.9, 12.2)	
16	3.95, dt (6.9, 8.8)	63.1
	4.07, ddd (2.6, 6.9, 8.3)	

Abbreviations: d, doublet; ddd, double double doublet; dt, double triplet; m, multiplet; s, singlet.

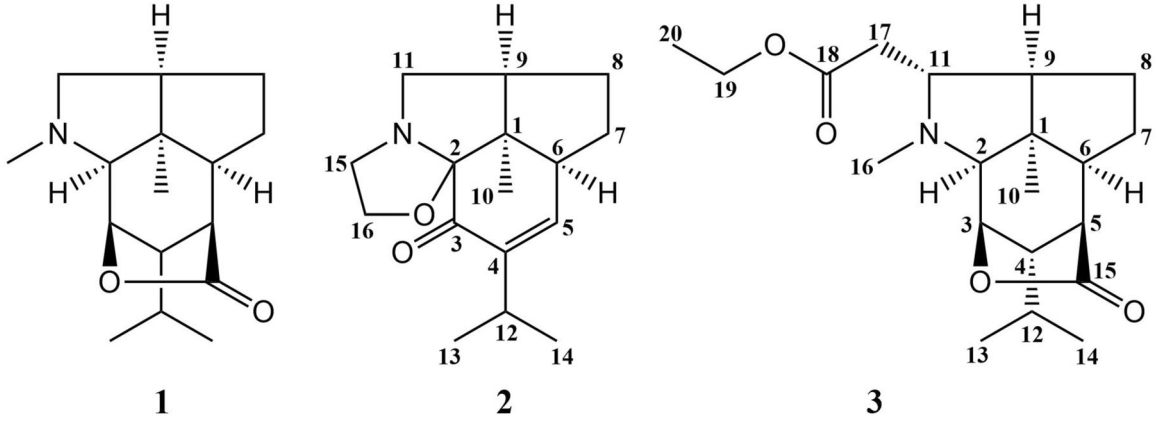

FIGURE 1 Structure of compounds **1**–**3** from *D. nobile* Lindl.

confirmed that C-2 of **2** was substituted with an oxazolidine moiety (Figure 2). An α, β-unsaturated carbonyl moiety was established by one carbonyl carbon and two olefinic carbons, which was confirmed by the HMBC correlations of H-5, H-12/C-3, and H_3-13, H_3-14/C-4 (Figure 2). The ROESY correlations of H-6/H-9/Me-10 suggested that these groups were α-oriented (Guo et al., 2018). Despite the presence of four asymmetric carbon atoms at C-1/C-2/C-6/C-9, the specific rotation of **2** was almost zero, suggesting it was a racemic mixture. Due to limited amount of compound **2**, its pure enantiomers were not obtained. Thus, compound **2** was elucidated and named as dendroxine B.

Compound **3** possessed a molecular formula of $C_{20}H_{31}NO_4$ according to HR-ESI-MS $[M+Na]^+$ (*m/z* 372.2148, calcd. 372.2146). The ^1H and ^{13}C NMR spectra of compound **3** demonstrated 20 signals, including three quaternary carbons (two carbonyl carbons, 172.1 ppm, 179.2 ppm), eight methines, four methylenes and five methyls (one N-CH_3), which were supported by the HSQC spectra (Table 3). These data suggested that **3** was similar to denrine (M. S. Zhang, Linghu et al., 2021), and the main difference was at C-11. Compared to denrine, the HMBC correlations of H-11/C-18, and H_2-17/C-11, C-18, and H_2-19/C-18, C-20 confirmed that C-11 of **3** was substituted with a 2-ethoxy-2-oxoethyl. The ROESY correlations of H-2/H-6/H-9/Me-10/H-12/H-17 suggested that these groups were α-oriented (Figure 2). The absolute structure of **3** was assigned as (1 R, 2 S, 3 R, 4 S, 5 R, 6 S, 9 S, 11 R) by ECD calculation (Figure 3). Thus, compound **3** was elucidated and named as denrine B.

3.2 | Compounds 1–3 protected PC12 cells from $A\beta_{1-42}$-induced neurotoxicity

The survival of PC12 cells for compounds **1**–**3** without or with $A\beta_{1-42}$ was evaluated by a CCK-8 assay. 0.001, 0.01, 0.1, and 1 μM of compounds **1**–**3** showed no cytotoxicity on undifferentiated PC12 cells (Supporting Information: Figure S1). Based on Figure 4, 0.001, 0.01, and 0.1 μM of compounds **1**–**3** exhibited no cytotoxic effects on differentiated PC12 cells (Supporting Information: Figure S2), but compound **2** reduced the viability of differentiated PC12 cells at 1 μM. Therefore, we chose 0.001, 0.01, and 0.1 μM of compounds **1**–**3** to treat differentiated PC12 cells in subsequent experiments.

As shown in Figure 4, 20 μM $A\beta_{1-42}$ markedly reduced the cell viability rate to 67.8% ± 2.3%. However, pretreatment with compounds **1**–**3** reversed this effect, compared to the $A\beta_{1-42}$ group. Pretreatment with 0.01 and 0.1 μM of compound **1** significantly increased the cell survival rate to 75.6% ± 2.5% and 80.2% ± 2.7%, respectively. Pretreatment with 0.01 and 0.1 μM of compound **2** enhanced the cell viability rate to 74.8% ± 2.5% and 77.8% ± 2.6%, respectively. Pretreatment with 0.1 μM of compound **3** increased the cell viability rate to 75.1% ± 2.5%. Pretreatment with memantine (0.1 μM) enhanced the cell survival rate to

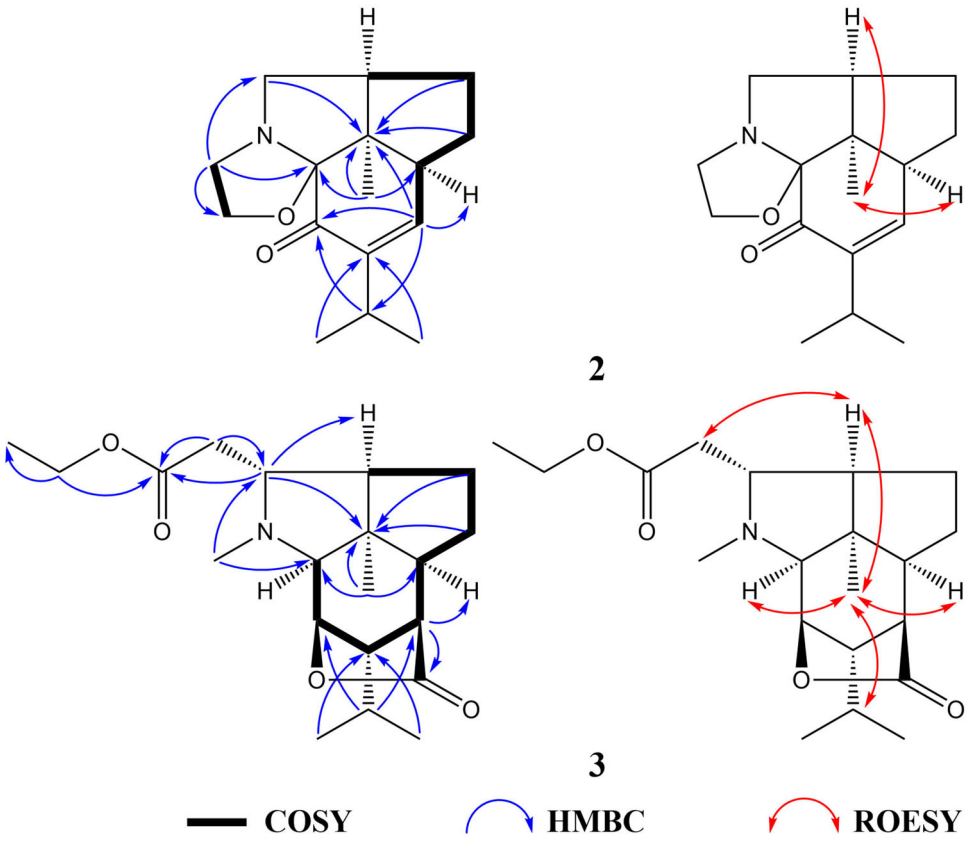

FIGURE 2 Key ^1H-^1H COSY, HMBC and ROESY correlations of compound **2** and **3**

TABLE 3 ^{1}H and ^{13}C NMR data of compound **3** (δ in ppm, J in Hz)

Position	δ_H	δ_C
1		50.5
2	2.83, d (2.8)	67.8
3	4.87, dd (2.8, 5.6)	79.2
4	2.11, m	51.5
5	2.43, dd (4.6, 5.8)	44.2
6	1.97, m	43.1
7	2.02, m	32.8
	2.09, m	
8	1.58, m	30.8
	1.84, m	
9	2.18, dt (7.3, 9.5)	60.5
10	1.36, s	33.0
11	3.11, ddd (3.8, 7.3, 8.5)	69.2
12	1.75, m	24.7
13	0.95, d (6.5)	20.5
14	0.96, d (6.5)	21.3
15		179.2
16	2.44, s	34.0
17	2.16, dd (8.8, 13.4)	40.6
	2.67, dd (3.9, 13.4)	
18		172.1
19	4.08, dq (7.1, 10.8)	60.4
	4.11, dq (7.1, 10.8)	
20	1.24, t (7.2)	14.4

Note: ^{1}H was recorded at 500 MHz and ^{13}C was recorded at 125 MHz in $CDCl_3$.

Abbreviations: d, doublet; dd, double doublet; dq, double quartet; dt, double triplet; m, multiplet; s, singlet.

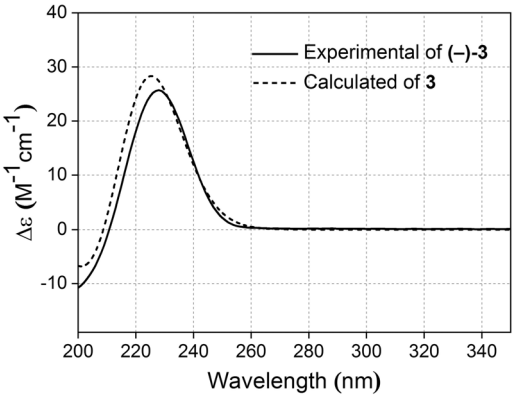

FIGURE 3 Calculated and experimental ECD spectra of compound **3**. ECD, electronic circular dichroism.

80.7% ± 2.7%. Thus, compounds **1**–**3** protected PC12 cells against $A\beta_{1-42}$-induced toxicity, among which dendrobine exhibited the greatest neuroprotective effect.

3.3 | Dendrobine attenuated $A\beta_{1-42}$-induced apoptosis in PC12 cells

The microscopic images of PC12 cells pretreated with dendrobine were shown in Figure 5. It can be seen that the cells exposure to $A\beta_{1-42}$ were rounder, more shrunken, and had an absence of neurites, when compared to the control group. Dendrobine pretreatment markedly reduced cell rounding and increased the cell population, and cell-to-cell contact, as compared to $A\beta_{1-42}$-treated cells.

Neuronal apoptosis was assessed by changes in nuclear morphological characteristics through a Hoechst 33342/PI staining assay. The nuclear structure of PC12 cells in the control group or dendrobine-treated group was round and without condensation, suggesting that there were no apoptotic cells (Figure 6). Compared to the control group, 20 μM $A\beta_{1-42}$ induced nuclear condensation, and enhanced the proportion of apoptotic cells to 15.8% ± 2.3%. However, pretreatment with dendrobine at 0.01 μM and 0.1 μM resulted in reduced cell apoptosis (10.4% ± 2.2% and 7.1% ± 2.6%, respectively) compared with $A\beta_{1-42}$-treated cells. By contrast, memantine reduced the cell apoptosis rate to 6.8% ± 2.1%.

3.4 | Dendrobine regulated the expression of Bcl-2, bax, cyto-c, and caspase-3 in $A\beta_{1-42}$-induced PC12 cells

As shown in Figures 7 and 8, $A\beta_{1-42}$ significantly decreased Bcl-2 mRNA and protein expression, but enhanced Bax, cyto-c, caspase-3 mRNA and protein expression in PC12 cells. However, compared with the $A\beta_{1-42}$ group, pretreatment with dendrobine reversed these effects, upregulated the Bcl-2 expression, but downregulated the Bax, cyto-c and caspase-3 expression. Taken together, dendrobine alleviated $A\beta_{1-42}$-induced apoptosis via the regulation of Bcl-2, Bax, cyto-c and caspase-3 expression in PC12 cells.

3.5 | Dendrobine inhibited CDK5 activation in $A\beta_{1-42}$-induced PC12 cells

We further determined the expression and phosphorylation of CDK5 to investigate the antiapoptosis mechanism of dendrobine. As shown in Figure 9, compared to the control group, $A\beta_{1-42}$ markedly caused an increase in the expression of CDK5 mRNA and protein, as well as the phosphorylation of CDK5 at Tyr15. In contrast, dendrobine pretreatment downregulated the expression of CDK5 and decreased the level of phosphorylated CDK5 at Tyr15, compared to those in the $A\beta_{1-42}$ group. These results indicated that dendrobine suppressed the activation of CDK5 in $A\beta_{1-42}$-treated PC12 cells.

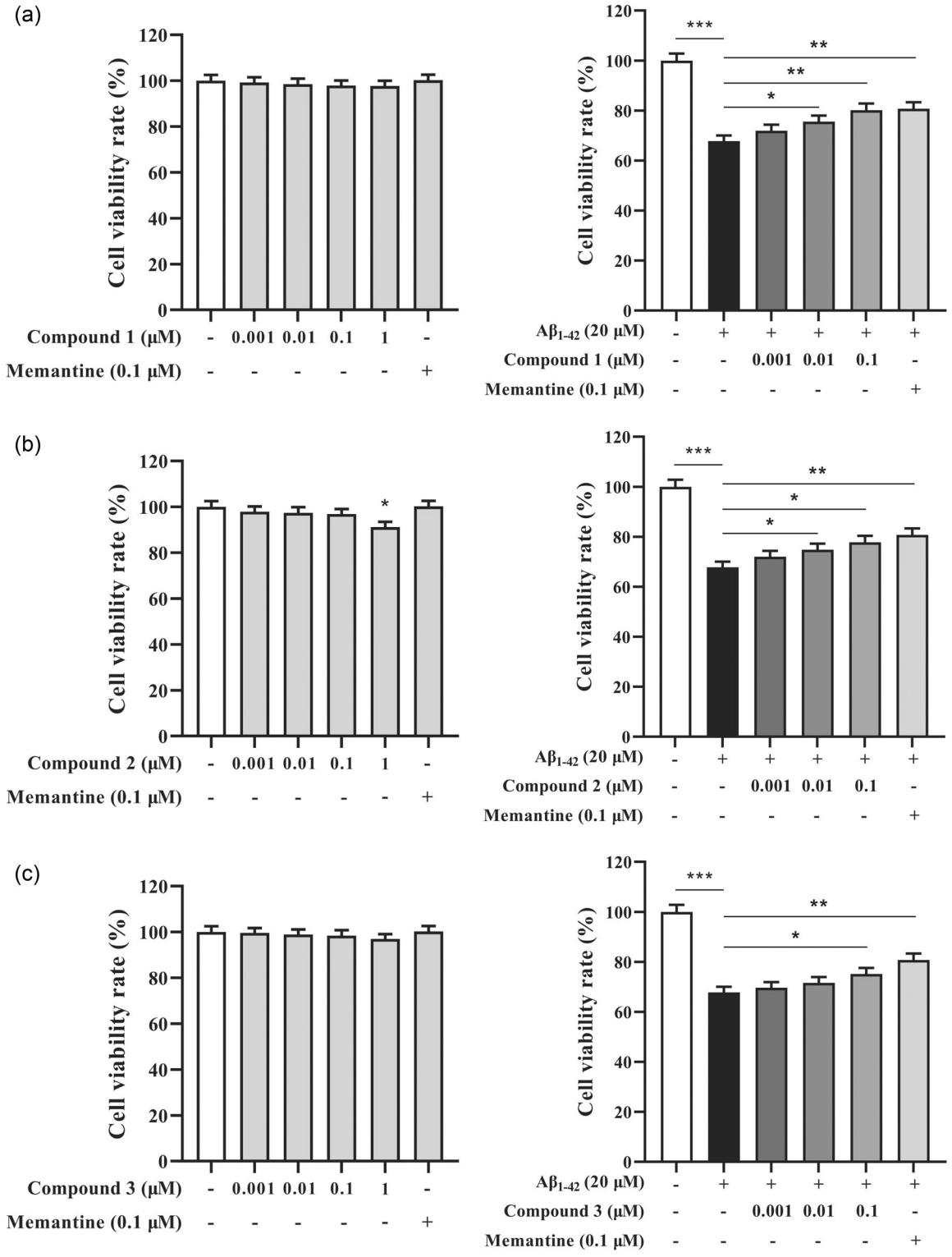

FIGURE 4 Effect on the survival of PC12 cells for compounds **1**–**3** without or with $A\beta_{1\text{-}42}$. ($n = 3$; $^{*}p < .05$, $^{**}p < .01$ and $^{***}p < .001$).

Molecular docking was conducted between dendrobine and human CDK5. Based on Figure 10, the hydrophobic interactions in the binding site were formed between dendrobine and CDK5. The cyclopentyl of dendrobine formed alkyl interactions with the residues of Ala31, Leu133, Ala143, Val64, Lys33, and Val18 in CDK5 and π-alkyl interaction with the benzene ring of Phe80 in CDK5. The carbon atom in the methyl of dendrobine formed alkyl interactions with the residues of Val18 and Ile10 in CDK5. VDW interactions were also formed between dendrobine and CDK5. The calculated docking score for dendrobine with CDK5 was −6.68 kcal/mol. As

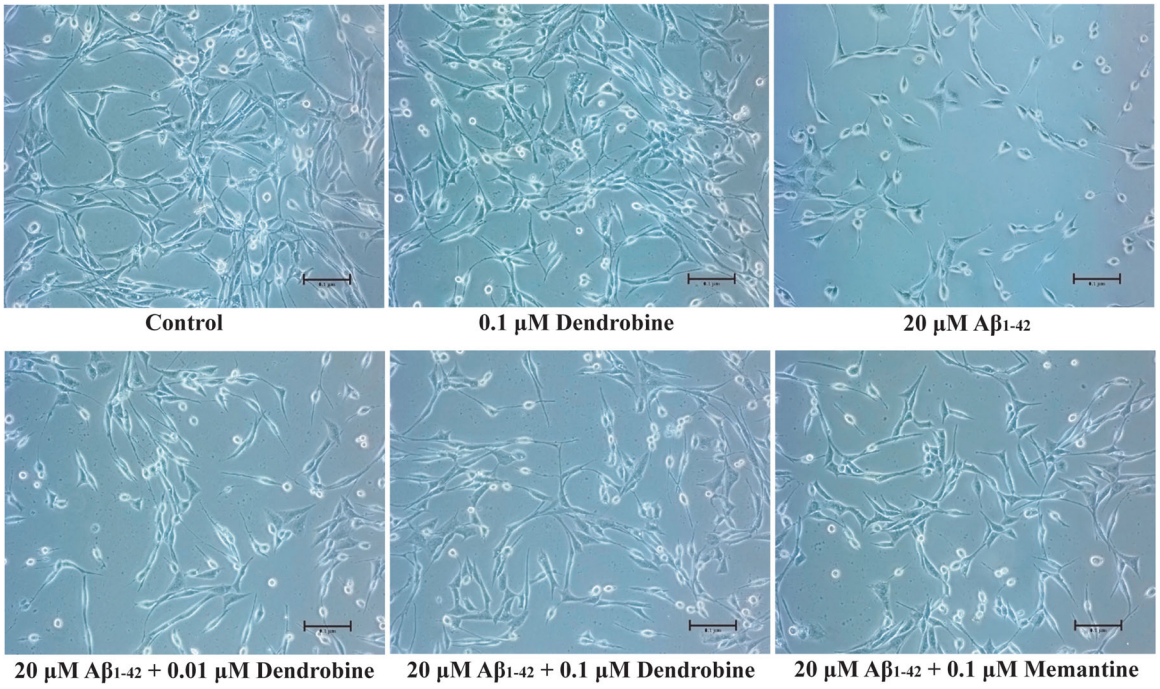

FIGURE 5 Effect of dendrobine on the morphology in $A\beta_{1-42}$-treated PC12 cells; scale bars = 0.1 μm

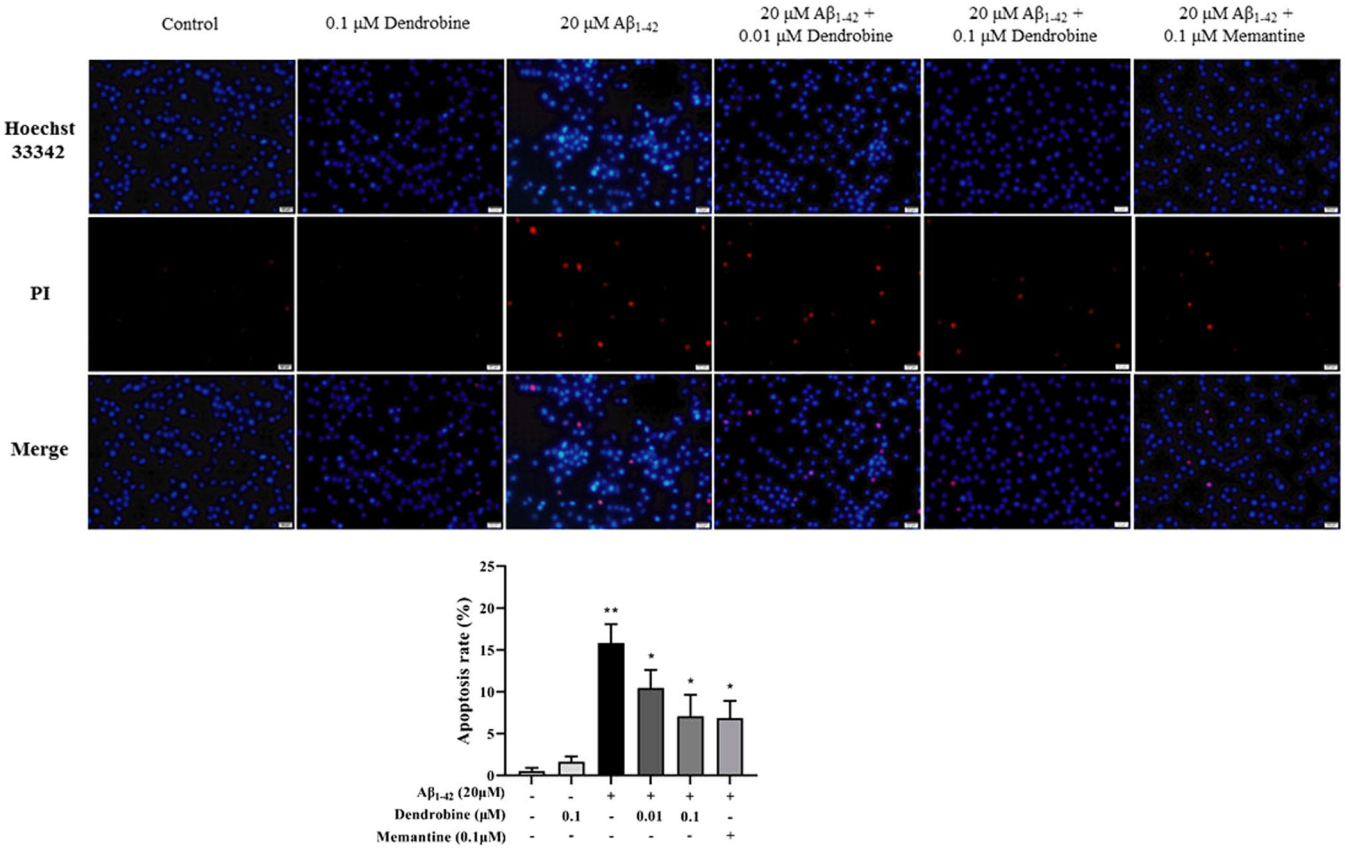

FIGURE 6 Effect of dendrobine on $A\beta_{1-42}$-induced apoptosis in PC12 cells. The bright blue fluorescent cells are early apoptotic cells, whereas the red fluorescent cells are late apoptotic or dead cells. Other cells with a less intense blue fluorescence are live cells. scale bars = 20 μm. ($n = 3$; $^{*}p < .05$, $^{**}p < .01$).

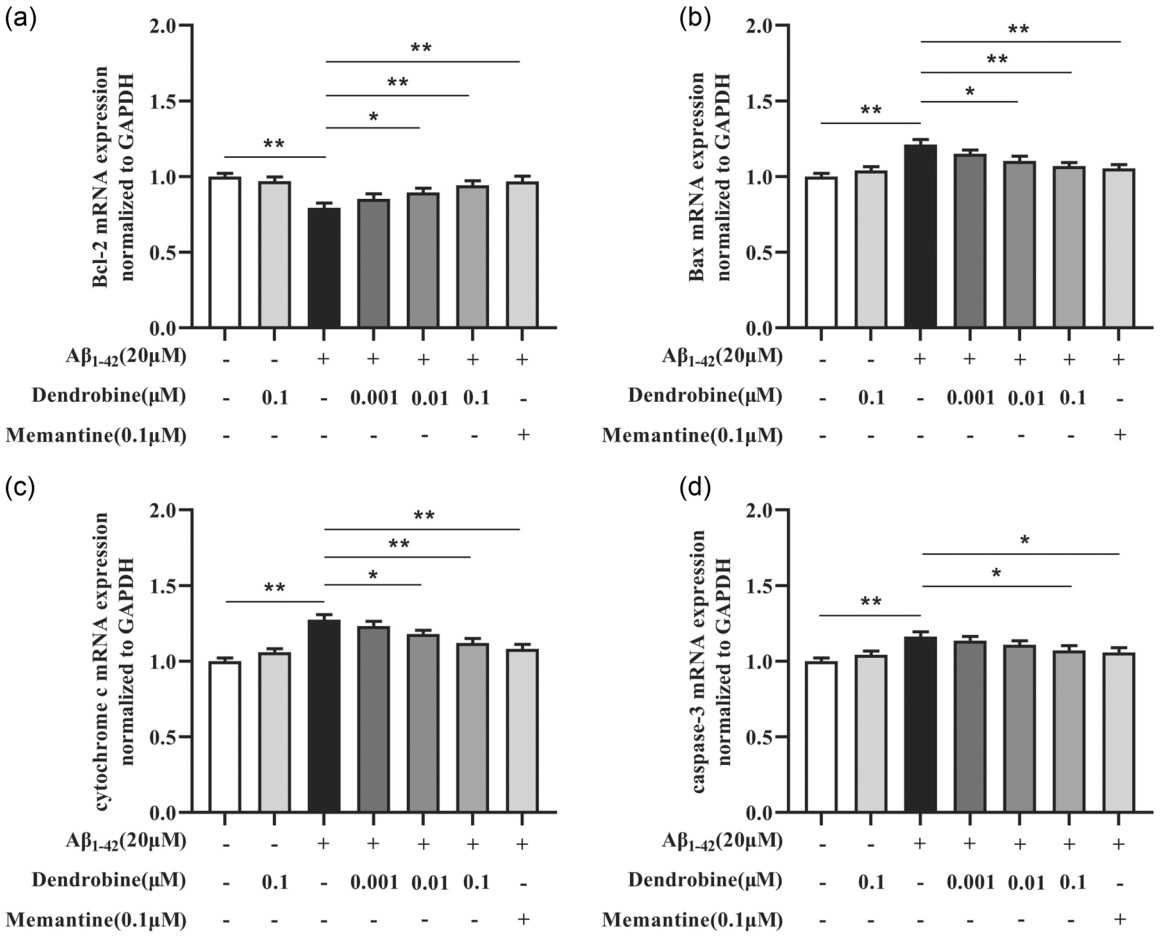

FIGURE 7 Effects of dendrobine on *Bcl-2*, *Bax*, *cyto-c*, and *caspase-3* mRNA expression in $A\beta_{1-42}$ treated PC12 cells (a–d). ($n = 3$; $^{*}p < .05$, $^{**}p < .01$). mRNA, messenger RNA.

shown in Supporting Information: Figure S3, the amino of memantine formed two hydrogen bonds with the residues of Glu51 and Asp144 in CDK5. The carbon atoms of memantine formed hydrophobic interactions with the residues of Val18, Ala31, Lys33, Val64, Phe80, Leu133, and Ala143 in CDK5. The calculated docking score for memantine with CDK5 was −7.50 kcal/mol. The result suggested that dendrobine could be docked into the binding site of CDK5.

To confirm the direct interaction between dendrobine and human CDK5 protein, the binding affinity of dendrobine with CDK5 protein was detected by a SPR assay. As shown in Figure 11, dendrobine interacted with CDK5 protein with a KD value of 2.05×10^{-4} M. The result showed that there is an affinity between dendrobine and human CDK5 protein.

4 | DISCUSSION

Aβ oligomers cause apoptosis, which finally results in neuronal death (Madhu & Mukhopadhyay, 2021). Therefore, prevention of neuronal apoptosis is considered to be a therapeutic strategy for AD. Drugs from natural bioactive substances have potential as treatments for AD (Chen et al., 2020). In the current study, three alkaloids, including two new compounds (dendroxine B, denrine B) and dendrobine, were isolated from *D. nobile* Lindl. and elucidated by spectroscopic analyses. An AD-like cell model was established using $A\beta_{1-42}$-induced PC12 cells to examine the effects on cell viability of compounds **1**–**3**. The neuroprotective mechanism of dendrobine in $A\beta_{1-42}$-induced PC12 cells was further investigated. For the first time, we demonstrated that compounds **1**–**3** show potent protective effects against $A\beta_{1-42}$-induced PC12 cell toxicity, with dendrobine showing the greatest neuroprotective effect; and the neuroprotective mechanism of dendrobine was mediated by inhibiting apoptosis via the regulation of CDK5 activation.

The pathological mechanism for AD is associated with neuronal apoptosis (Moujalled et al., 2021). Treatment with $A\beta_{1-42}$ induces downregulation of Bcl-2/Bax signaling, release of cyto-c, and activation of caspase-3 (Moujalled et al., 2021). In the previous study, DNLA protected rat cortical and hippocampal neurons from $A\beta_{25-35}$-induced neurotoxicity (W. Zhang et al., 2017; W. Zhang et al., 2022), and inhibited $A\beta_{25-35}$-induced PC12 cell apoptosis (Y. Liu et al., 2021). In current study, we

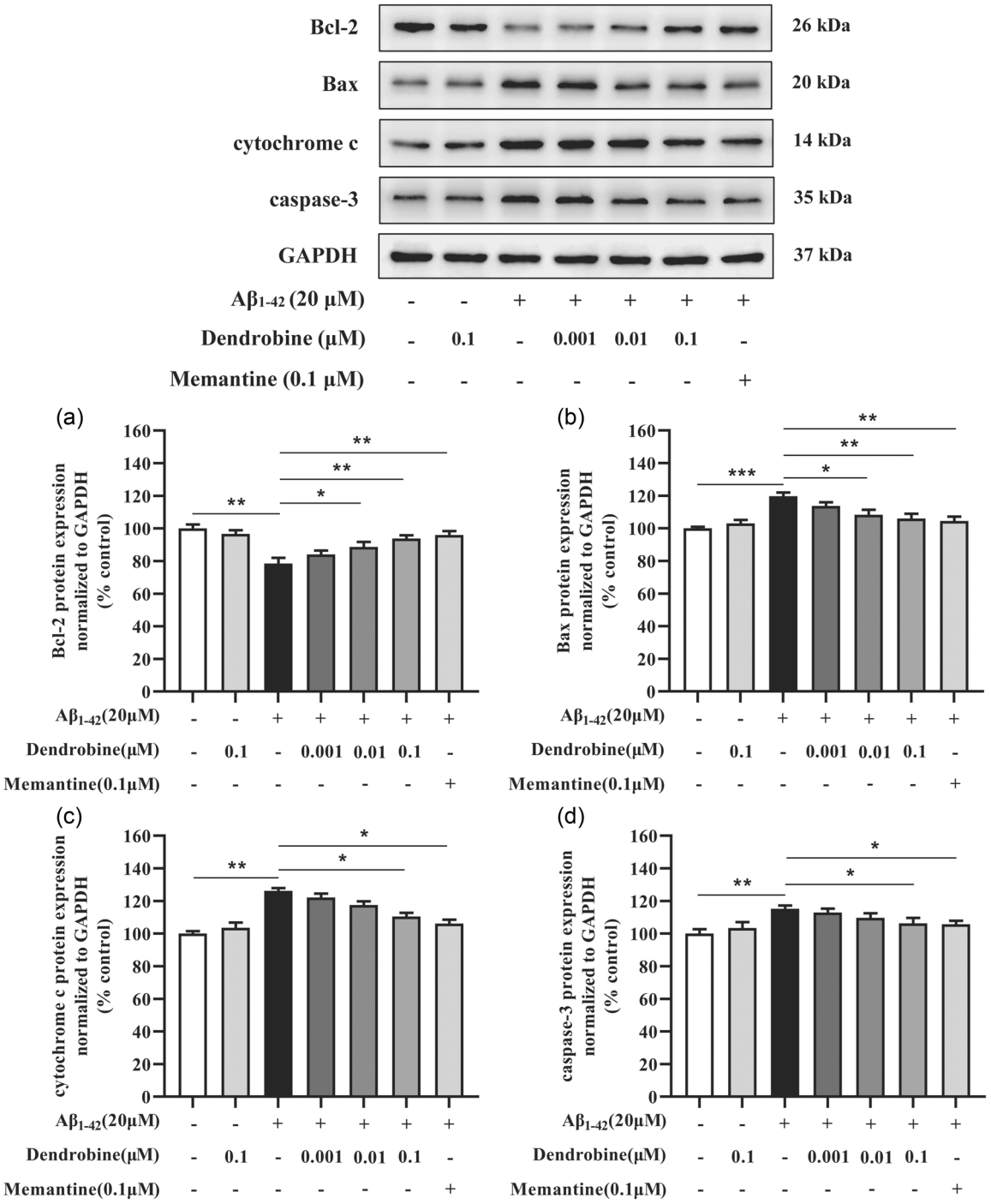

FIGURE 8 Effects of dendrobine on Bcl-2, Bax, cyto-c, and caspase-3 protein expression in $A\beta_{1-42}$ treated PC12 cells (a–d). ($n = 3$; $^{*}p < .05$, $^{**}p < .01$ and $^{***}p < .001$).

found that dendrobine suppressed $A\beta_{1-42}$-induced apoptosis signaling pathway in PC12 cells. Dendrobine pretreatment reduced the proportion of early and late apoptotic cells, increased Bcl-2 expression, and decreased Bax, cyto-c, and caspase-3 expression in $A\beta_{1-42}$-induced PC12 cells.

Amyloid-β activates cell cycle pathways involving CDKs, leading to the upregulation of GSK-3β and hyperphosphorylation of tau protein (M. S. Zhang, Linghu, et al., 2021; Y. Zhang, Zhang, et al., 2021). Aβ induces neurotoxicity via enhanced CDK5 activity (S. L. Liu et al., 2016). The overactivation of CDK5 contributes to neuronal cell apoptosis in AD (Lu et al., 2019). Inhibition of CDK5 promoted Bcl-2 expression, reduced Bax and caspase-3 expressions (S. L. Liu et al., 2016). Administration of CDK inhibitor flavopiridol reverses memory impairment in the AD mouse model induced by $A\beta_{1-42}$ (Malhotra et al., 2021). Pretreatment with dendrobine not only decreased the expression of CDK5 but also suppressed the phosphorylation of CDK5 at Tyr15 in $A\beta_{1-42}$-induced

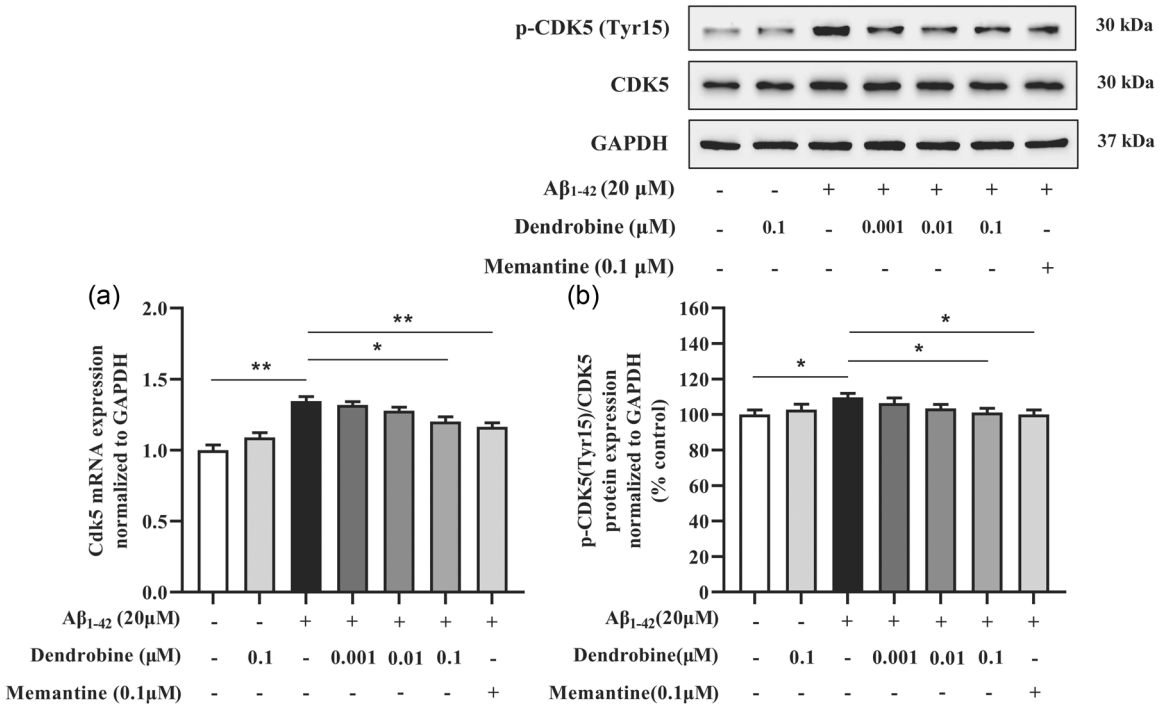

FIGURE 9 Effect of dendrobine on the mRNA expression of *Cdk5* (a) and protein expression of p-CDK5 (Tyr15) and CDK5 (b) in $A\beta_{1-42}$-treated PC12 cells. ($n = 3$; $^{*}p < .05$, $^{**}p < .01$). mRNA, messenger RNA.

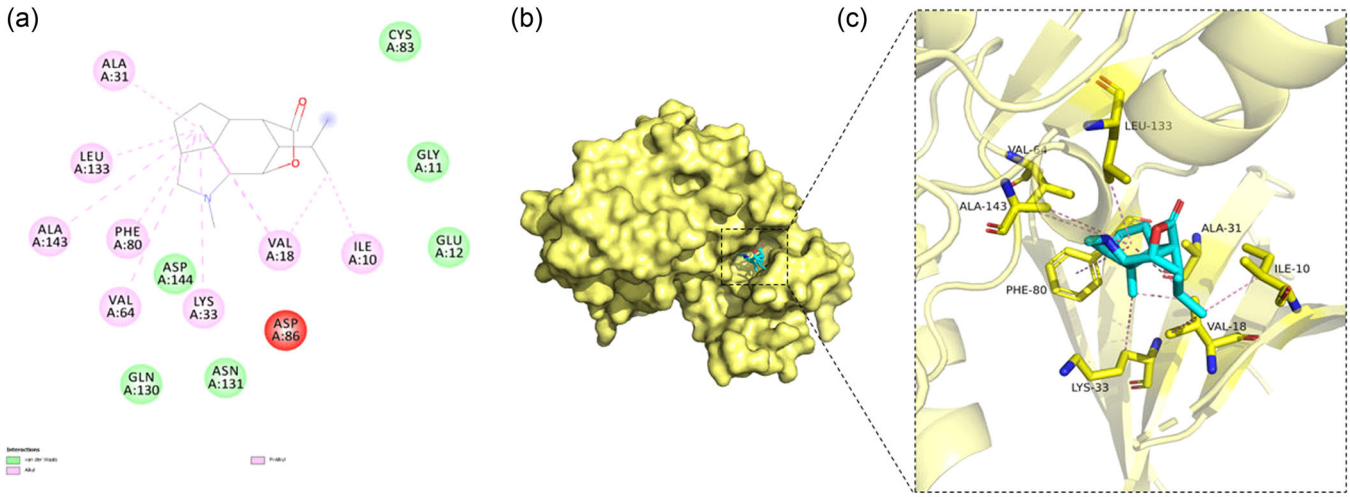

FIGURE 10 The molecular docking result of dendrobine with CDK5 (PDB ID: 7VDP). (a) The two-dimensional interaction diagram of dendrobine and CDK5. (b) The surface binding mode of dendrobine (cyan stick) and CDK5 (yellow). (c) The three-dimensional interaction diagram of dendrobine and CDK5. The pink dotted lines indicated the formation of the hydrophobic interactions.

PC12 cells, thereby inhibiting $A\beta_{1-42}$-induced CDK5 activation. The results showed that dendrobine directly bound to human CDK5 protein with a KD value of 2.05×10^{-4} M.

Until now, the neuroprotective activity of dendrobine in animal models of AD remains unclear, which is a limitation of this study. Therefore, the safety and effectiveness of dendrobine against AD will be confirmed using animal models in further experimental research.

5 | CONCLUSIONS

In summary, two new alkaloids (dendroxine B and denrine B) and dendrobine, were isolated from the EtOH extract of *D. nobile* Lindl. stems. The current research demonstrated that two new alkaloids and dendrobine protected PC12 cells against $A\beta_{1-42}$-induced neurotoxicity for the first time, among which dendrobine showed the greatest neuroprotective effect. Regarding the mechanism,

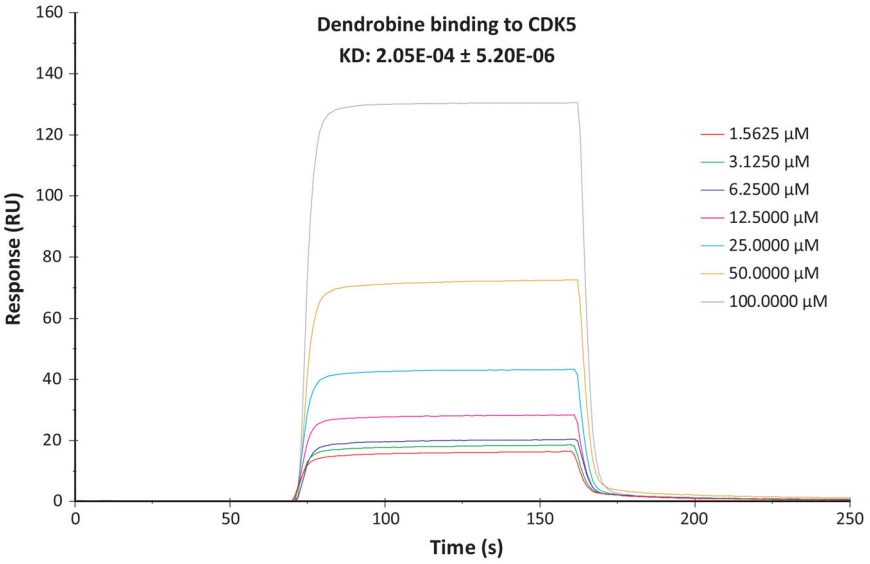

FIGURE 11 The binding affinity of dendrobine with human CDK5 protein was evaluated using a SPR assay with CDK5 immobilized on a sensor chip. Varied concentrations of dendrobine were detected with the binding affinity analyzed by Biacore Evaluation software ($n = 3$). Data shown are means ± SEM. SPR, surface plasmon resonance.

dendrobine attenuated $A\beta_{1-42}$-induced apoptosis by suppressing the activation of CDK5 in PC12 cells.

ACKNOWLEDGMENTS

This research was supported by the Science and Technology Department of Guizhou Province (No. QKHJC-ZK[2021]YB567, QKHRCPT[2017]5101, and QKHRCPT[2017]5733-061); the State Key Laboratory of Functions and Applications of Medicinal Plants, Guizhou Medicial University (No. FAMP201910K).

CONFLICT OF INTEREST

The authors declare no conflict of interest.

DATA AVAILABILITY STATEMENT

The data that supports the findings of this study are available in the supplementary material of this article

ORCID

Cheng-Chen Zhang http://orcid.org/0000-0002-5477-3258

REFERENCES

Alghazwi, M., Smid, S., Musgrave, I., & Zhang, W. (2019). In vitro studies of the neuroprotective activities of astaxanthin and fucoxanthin against amyloid beta ($A\beta_{1-42}$) toxicity and aggregation. *Neurochemistry International*, *124*, 215–224. https://doi.org/10.1016/j.neuint.2019.01.010

Chen, S. Y., Gao, Y., Sun, J. Y., Meng, X. L., Yang, D., Fan, L. H., Xiang, L., & Wang, P. (2020). Traditional Chinese Medicine: Role in reducing β-amyloid, apoptosis, autophagy, neuroinflammation, oxidative stress, and mitochondrial dysfunction of Alzheimer's Disease. *Frontiers in Pharmacology*, *11*, 497. https://doi.org/10.3389/fphar.2020.00497

Cummings, J., Lee, G., Zhong, K., Fonseca, J., & Taghva, K. (2021). Alzheimer's disease drug development pipeline: 2021. *Alzheimer's & dementia (New York, N. Y.)*, *7*(1), 12179. https://doi.org/10.1002/trc2.12179

Guo, L., Frey, W., & Plietker, B. (2018). Catalytic enantioselective total synthesis of the picrotoxane alkaloids (-)-dendrobine, (-)-mubironine B, and (-)-dendroxine. *Organic Letters*, *20*(14), 4328–4331. https://doi.org/10.1021/acs.orglett.8b01782

Hu, M., Liu, Y., He, L., Yuan, X., Peng, W., & Wu, C. (2019). Antiepileptic effects of protein-rich extract from *Bombyx batryticatus* on mice and its protective effects against H_2O_2-Induced oxidative damage in PC12 cells via regulating PI3K/Akt signaling pathways. *Oxidative Medicine and Cellular Longevity*, *2019*, 1–13. https://doi.org/10.1155/2019/7897584

Li, D. D., Zheng, C. Q., Zhang, F., & Shi, J. S. (2022). Potential neuroprotection by *Dendrobium nobile* Lindl alkaloid in Alzheimer's disease models. *Neural Regeneration Research*, *17*(5), 972–977. https://doi.org/10.4103/1673-5374.324824

Liu, S. L., Wang, C., Jiang, T., Tan, L., Xing, A., & Yu, J. T. (2016). The role of Cdk5 in Alzheimer's Disease. *Molecular Neurobiology*, *53*(7), 4328–4342. https://doi.org/10.1007/s12035-015-9369-x

Liu, Y., Pi, T., Yang, X., & Shi, J. (2021). Protective effects and mechanisms of *Dendrobium nobile* Lindl. alkaloids on PC12 cell damage induced by $A\beta_{25-35}$. *Behavioural Neurology*, *2021*, 1–11. https://doi.org/10.1155/2021/9990375

Long, J. M., & Holtzman, D. M. (2019). Alzheimer disease: An update on pathobiology and treatment strategies. *Cell*, *179*(2), 312–339. https://doi.org/10.1016/j.cell.2019.09.001

Lu, T. T., Wan, C., Yang, W., & Cai, Z. (2019). Role of Cdk5 in amyloid-beta pathology of Alzheimer's disease. *Current Alzheimer Research*, *16*(13), 1206–1215. https://doi.org/10.2174/1567205016666191210094435

Madhu, P., & Mukhopadhyay, S. (2021). Distinct types of amyloid-β oligomers displaying diverse neurotoxicity mechanisms in Alzheimer's disease. *Journal of Cellular Biochemistry*, *122*(11), 1594–1608. https://doi.org/10.1002/jcb.30141

Malhotra, N., Gupta, R., & Kumar, P. (2021). Pharmacological relevance of CDK inhibitors in Alzheimer's disease. *Neurochemistry International*, *148*, 105115. https://doi.org/10.1016/j.neuint.2021.105115

Michaels, T. C. T., Šarić, A., Curk, S., Bernfur, K., Arosio, P., Meisl, G., Dear, A. J., Cohen, S. I. A., Dobson, C. M., Vendruscolo, M., Linse, S., & Knowles, T. P. J. (2020). Dynamics of oligomer populations formed during the aggregation of Alzheimer's Aβ42 peptide. *Nature Chemistry*, *12*(5), 445–451. https://doi.org/10.1038/s41557-020-0452-1

Miranda, A., Montiel, E., Ulrich, H., & Paz, C. (2021). Selective secretase targeting for Alzheimer's disease therapy. *Journal of Alzheimer's Disease*, *81*(1), 1–17. https://doi.org/10.3233/jad-201027

Moujalled, D., Strasser, A., & Liddell, J. R. (2021). Molecular mechanisms of cell death in neurological diseases. *Cell Death and Differentiation*, *28*(7), 2029–2044. https://doi.org/10.1038/s41418-021-00814-y

Nie, X., Chen, Y., Li, W., & Lu, Y. (2020). Anti-aging properties of *Dendrobium nobile* Lindl.: From molecular mechanisms to potential treatments. *Journal of Ethnopharmacology*, *257*, 112839. https://doi.org/10.1016/j.jep.2020.112839

Ospondpant, D., Gao, X., Dong, T. T., & Tsim, K. W. K. (2022). Dracaena cochinchinensis stemwood extracts inhibit amyloid-β fibril formation and promote neuronal cell differentiation. *Frontiers in Pharmacology*, *13*, 943638. https://doi.org/10.3389/fphar.2022.943638

Quntanilla, R. A., & Tapia-Monsalves, C. (2020). The role of mitochondrial impairment in Alzheimer's disease neurodegeneration: The tau connection. *Current Neuropharmacology*, *18*(11), 1076–1091. https://doi.org/10.2174/1570159x18666200525020259

Sharma, V. K., Singh, T. G., Singh, S., Garg, N., & Dhiman, S. (2021). Apoptotic pathways and Alzheimer's disease: Probing therapeutic potential. *Neurochemical Research*, *46*(12), 3103–3122. https://doi.org/10.1007/s11064-021-03418-7

Tu, S., Okamoto, S., Lipton, S. A., & Xu, H. (2014). Oligomeric Aβ-induced synaptic dysfunction in Alzheimer's disease. *Molecular Neurodegeneration*, *9*, 48. https://doi.org/10.1186/1750-1326-9-48

Wang, Y. H. (2021). Traditional uses, chemical constituents, pharmacological activities, and toxicological effects of *Dendrobium* leaves: A review. *Journal of Ethnopharmacology*, *270*, 113851. https://doi.org/10.1016/j.jep.2021.113851

Yang, D., Cheng, Z. Q., Hou, B., Yang, L., Zi, C. T., Dong, F. W., Hu, J. M., & Zhou, J. (2020). Two unusual dendrobine-type alkaloids from *Dendrobium findlayanum*. *Fitoterapia*, *144*, 104607. https://doi.org/10.1016/j.fitote.2020.104607

Yang, D., Wu, W., Gan, G., Wang, D., Gong, J., Fang, K., & Lu, F. (2020). (-)-Syringaresinol-4-O-β-D-glucopyranoside from *Cortex Albizziae* inhibits corticosterone-induced PC12 cell apoptosis and relieves the associated dysfunction. *Food and Chemical Toxicology*, *141*, 111394. https://doi.org/10.1016/j.fct.2020.111394

Zeng, Q., Zhou, Y., Liang, D., He, H., Liu, X., Zhu, R., Zhang, M., Luo, X., Wang, Y., & Huang, G. (2020). Exosomes secreted from bone marrow mesenchymal stem cells attenuate oxygen-glucose deprivation/reoxygenation-induced pyroptosis in PC12 cells by promoting AMPK-dependent autophagic flux. *Frontiers in Cellular Neuroscience*, *14*, 182. https://doi.org/10.3389/fncel.2020.00182

Zhang, M. S., Linghu, L., Wang, G., He, Y. Q., Sun, C. X., & Xiao, S. J. (2021). Dendrobine-type alkaloids from *Dendrobium nobile*. *Natural Product Research*, *36*, 5393–5399. https://doi.org/10.1080/14786419.2021.2019731

Zhang, W., Wu, Q., Lu, Y., Gong, Q., Zhang, F., & Shi, J. (2017). Protective effects of *Dendrobium nobile* Lindl. alkaloids on amyloid beta (25-35)-induced neuronal injury. *Neural Regeneration Research*, *12*(7), 1131–1136. https://doi.org/10.4103/1673-5374.211193

Zhang, W., Zhang, M., Wu, Q., & Shi, J. (2022). *Dendrobium nobile* Lindl. alkaloids ameliorate Aβ25-35-induced synaptic deficits by targeting Wnt/β-catenin pathway in Alzheimer's Disease models. *Journal of Alzheimer's Disease*, *86*(1), 297–313. https://doi.org/10.3233/jad-215433

Zhang, Y., Zhang, Y., Aman, Y., Ng, C. T., Chau, W. H., Zhang, Z., Yue, M., Bohm, C., Jia, Y., Li, S., Yuan, Q., Griffin, J., Chiu, K., Wong, D. S. M., Wang, B., Jin, D., Rogaeva, E., Fraser, P. E., Fang, E. F., … Song, Y. Q. (2021). Amyloid-β toxicity modulates tau phosphorylation through the PAX6 signalling pathway. *Brain*, *144*, 2759–2770. https://doi.org/10.1093/brain/awab134

Zhang, Z., Xu, P., Yu, H., & Shi, L. (2019). Luteolin protects PC-12 cells from H_2O_2-induced injury by up-regulation of microRNA-21. *Biomedicine & Pharmacotherapy = Biomedecine & Pharmacotherapie*, *112*, 108698. https://doi.org/10.1016/j.biopha.2019.108698

SUPPORTING INFORMATION

Additional supporting information can be found online in the Supporting Information section at the end of this article.

How to cite this article: Zhang, C.-C., Kong, Y.-L., Zhang, M.-S., Wu, Q., & Shi, J.-S. (2023). Two new alkaloids from *Dendrobium nobile* Lindl. exhibited neuroprotective activity, and dendrobine alleviated $A\beta_{1-42}$-induced apoptosis by inhibiting CDK5 activation in PC12 cells. *Drug Development Research*, 84, 262–274. https://doi.org/10.1002/ddr.22030